Determining forest parameters for avalanche simulation using remote sensing data

Natalie Brožová[a],[*], Jan-Thomas Fischer[b], Yves Bühler[a], Perry Bartelt[a], Peter Bebi[a]

[a] *WSL Institute for Snow and Avalanche Research SLF, Davos Dorf, Switzerland*
[b] *Austrian Research Centre for Forests (BFW), Innsbruck, Austria*

ARTICLE INFO

ABSTRACT

Mountain forests offer effective, natural and cost-efficient protection against avalanches. Trees reduce the probability of an avalanche formation and can significantly decelerate small to medium size avalanches. Remote sensing methods enable an efficient assessment of forest structural parameters on large scale and therefore determine the protective capacity of a specific forest. The aims of this study are: (i) to evaluate the quality of forest structural parameters obtained from remote sensing data using two different methods; and (ii) to determine how forest parameters and forest cover changes influence avalanche runout. We compared the control assessment of maximum tree height and crown coverage in 107 plots (50 in evergreen and 57 in deciduous forests). The same parameters were analysed using (i) a photogrammetry-based vegetation height model (VHM$_P$) and (ii) a LiDAR-based vegetation height model (VHM$_L$). The control assessment of surface roughness was compared to the analysis of a digital terrain model (DTM). We then simulated two avalanche case studies near Davos (Switzerland) with forest parameters estimated by the remote sensing and control methods. Tree height and crown coverage assessed with both remote sensing methods (VHM$_P$ and VHM$_L$) did not differ significantly from the control measurements. However, surface roughness was underestimated. This had a significant influence on simulation results. For the first case study, a wet-snow avalanche, the simulated runout distances did not differ significantly, when using forest parameters from either of the two tested remote sensing methods. The simulated runout distance increased for an avalanche scenario with less forest cover in the release area and/or less forest cover after forest destruction by a preceding avalanche event. For the second case study, a dry-snow avalanche, the forest cover was underestimated by the VHM$_P$, which led to longer simulated runout distances. Our study indicates that available remote sensing methods are increasingly suitable for the determination of forest parameters which are relevant for avalanche simulation models. However, more research is needed on the precise estimation of forest cover in release areas and understanding how forest cover changes affect avalanche runout.

1. Introduction

Forests contribute in several ways to the mitigation of snow avalanches. Forests influence the snowpack structure and thereby hinder the avalanche release through interception, microclimate and higher surface roughness (Schneebeli and Bebi, 2004; McClung and Schaerer, 2006; Bebi et al., 2009; Teich et al., 2012). The capacity of slowing and stopping avalanches in the forest stand is less known (Feistl et al., 2014). This ability is limited, and large-scale, fast moving avalanches destroy the forest (Takeuchi et al., 2011; Feistl et al., 2015; Giacona et al., 2018). Small to medium size avalanches (corresponding to avalanche sizes 1–2; EAWS, 2012), which are often threats for roads and railways, can be stopped or their runout is shortened by the presence of

a forest (Teich et al., 2013b). The structure of mountain forests for mitigating avalanches in the release and runout zone is highly spatially variable and may also drastically change in time as a response to natural or anthropogenic forest cover changes (Bebi et al., 2001). Abrupt changes in forests have an effect on avalanche formation and runout. This is particularly important in the case of disturbance interactions or repeated avalanche disturbances. Frequent disturbances do not allow the regrowth of forests as in the case of avalanche tracks (Johnson, 1987). In order to better account for the spatial and temporal changes in forest cover in avalanche hazard mapping and risk analysis, it would therefore be highly valuable to compare the avalanche runout distances with changing forest cover. We expect that less forest cover leads to longer runout distance of an avalanche.

⁎ Corresponding author at: Flüelastrasse 11, 7260 Davos Dorf, Switzerland.
E-mail address: natalie.brozova@slf.ch (N. Brožová).

The representation of forest effects in currently used avalanche simulation tools is that the forest is taken into account to increase friction. This hardly represents spatial differences in forest structures and their effects on avalanche runout reduction (Feistl et al., 2014; Teich et al., 2013a). It is fundamental to gather forest parameters before initiating the simulation; currently, this is mostly done from remote sensing data, which is the most efficient and accurate method for quantifying forest biomass on a large scale. Remote sensing data is used, next to the other purposes, in forest inventory. Different platforms with different sensors deliver a variety of spatial resolution. This varies from very high resolution in the order of centimetres (UAS), to medium resolution in order of decimetres (airplane), or low resolution in the order of meters (satellites). Most of the present studies deal with the evaluation of LiDAR and photogrammetry methods for forestry applications (Lisein et al., 2013; Thiel and Schmullius, 2016; Gašparović et al., 2017; Ivosevic et al., 2017; Fankhauser et al., 2018), which belong to the methods able to deliver data with the highest resolution. Digital surface models (DSM) generated using photogrammetry or LiDAR methods have a great application in forest inventory, because they contain information about the height of vegetation in forests. By extracting the digital terrain model (DTM) the height of the vegetation can be calculated. This vegetation height model (VHM) can be applied in generating forest masks or extracting forest canopy gaps (Ginzler and Hobi, 2015), which is very important for the estimation of potential avalanche release areas (Bebi et al., 2001). Ginzler and Hobi (2015) have shown that the spatial resolution of VHM with DSM based on photogrammetry (VHM$_P$) was useful not for single-tree analyses, but for analysing entire forest stand. However, it is not clear, if high resolution remote sensing data (e.g. orthophoto, digital surface and terrain models, vegetation height models and other digital data) are able to deliver the necessary input accuracy of forest characteristics to get accurate simulation results of avalanches (Stritih et al., 2019). Forest structure and the effect of detrainment is considered in the latest scientific version of the simulation tool RAMMS "extended", module Avalanche (Rapid Mass Movement Simulation, version 2.7.29; Feistl et al., 2014). Therefore snow may be extracted from the avalanche, which leads to stopping or deceleration and runout shortening (Teich et al., 2012; Feistl et al., 2014; Teich et al., 2013a). Simulation of small to medium size forest avalanches was thus improved by including the detrainment coefficient K [kg m-1 s-2], which depends on forest parameters, such as forest type, crown coverage and surface roughness and respectively influencing the runout distance of the avalanche (Feistl et al., 2014; Teich et al., 2013a). In this paper, we present an analysis of remote sensing data obtained by different methods for the estimation of forest parameters; and the suitability for using these parameters for avalanche simulation. In this study we addressed the following research topics: (i) the effect of varying forest cover on the release and runout area and simulated avalanche runout distance, (ii) the comparison of single forest parameters (as maximum height, crown coverage and surface roughness) obtained from remote sensing methods, (iii) the effect of forest structure, defined by remote sensing methods, on the model parameters and the simulated runout distance of an avalanche, respectively.

2. Materials and methods

2.1. Field sites

We compared the assessment of LiDAR- and photogrammetry-based remote sensing methods for forest structural parameters with a field-based control method in a total of 107 study plots (50 plots in evergreen forest and 57 plots deciduous forest). These plots were collected during field campaigns in 2017 and 2018 at three regions in the canton Grisons (Switzerland), where high resolution LiDAR data and photogrammetry based vegetation height model was available (Fig. 1). The area around Davos is typical for evergreen forests (dominated by *Picea abies*);

Bündner Herrschaft and Schanfigg represent localities with a larger proportion of deciduous forests (composed by *Fagus sylvatica*, *Fraxinus excelsior* and other species). For all 107 plots, we measured tree height of the central tree and estimated surface roughness in two radii of 5 and 10 m. In each radius three highest roughness elements were recorded with the position from the central tree (distance and azimuth), its height and material. The crown coverage was estimated (in 5%-increments) in the field and from a high-resolution (0.25 m) orthophoto and compared to the LiDAR- and photogrammetry-based remote sensing data. These simulation input parameters are suggested in the look-up table from RAMMS (see Table 2; Feistl et al., 2014; Teich et al., 2013a; Feistl, 2015).

2.2. Remote sensing datasets

To compare the accuracy of forest parameters from different remote sensing methods with the control method, two vegetation height models were used (Table 1). (1) A first a vegetation height model (VHM$_P$) was calculated using a digital surface model (DSM) based on photogrammetry. Digital aerial summer images from the years 2011 to 2012 were used to calculate the DSM with resolution of 1 m. The difference between the digital surface model and the digital terrain model (DTM) based on laser data (provided by the Swiss Federal Office of Topography, with point density 0.5 points per m^2 and a resampled resolution of 1 m) produced the VHM$_P$ with resolution of 1 m (Ginzler and Hobi, 2015). (2) To produce the second vegetation height model (VHM$_L$), we combined both DSM and DTM based on LiDAR flight from August 2015. The resolution of the VHM$_L$ is 1 m (resampled from 0.5 m resolution and with point density 12 points per m^2). In order to avoid significant differences caused by the varying acquisition periods, we pre-selected with the help of forest stand maps and high resolution orthophotos (0.25 m) mainly adult trees with relatively slow growth dynamics in areas without forest intervention or visible natural disturbances.

Tree heights from VHM$_P$ and VHM$_L$ were calculated at each plot representing the maximum height value per plot with radius of 5 m, which would represent the size of a tree crown. These heights were compared to the heights measured in the field (using ultrasound instrument Vertex) in all 107 study plots. The normal distribution of differences (difference between the measured heights and heights from VHM$_P$ and VHM$_L$) was analysed using histograms with a superimposed curve, a Shapiro-Wilk test of normality and normal Q-Q plots (Höhle and Höhle, 2009). These tests revealed a non-normal distribution of the variation for both VHM$_P$ and VHM$_L$. Robust accuracy measures suited for non-normal distribution were therefore used. This included the normalized median absolute deviation (NMAD), 68.3% quantile and 95% quantile (Höhle and Höhle, 2009).

Crown coverage was compared on the level of study plots with 20 m radius for deciduous and evergreen forest types in three crown coverage classes: open (20%–40%), scattered (40%–70%) and dense (> 70%). In every forest type and every coverage class, crown coverage was analysed in 10 random plots (60 plots in total). Correlations were calculated between the single models, the control method (estimation of crown coverage from an orthophoto), and models together.

Surface roughness was calculated from DTM using a vector ruggedness measure developed by Sappington et al. (2007). To calculate the surface roughness, a window size had to be specified. We applied a window size of 5 pixels, which corresponds to 5 m at spatial resolution of 1 m. All normal vectors to the ground were analysed within this window and their deviation was calculated. The resulting layer was with values between 0 and 1. Three categories were used to classify the terrain roughness within the study plots: 1-smooth, 2-knobby and 3-rough, using thresholds 0.02 (smooth to knobby) and 0.03 (knobby to rough) for the calculated roughness from DTM (Fig. 7).

Surface roughness was analysed on the level of the study plots with two different radii (5 and 10 m) as well as on the single element level, together with the control method (observations and measurements in the
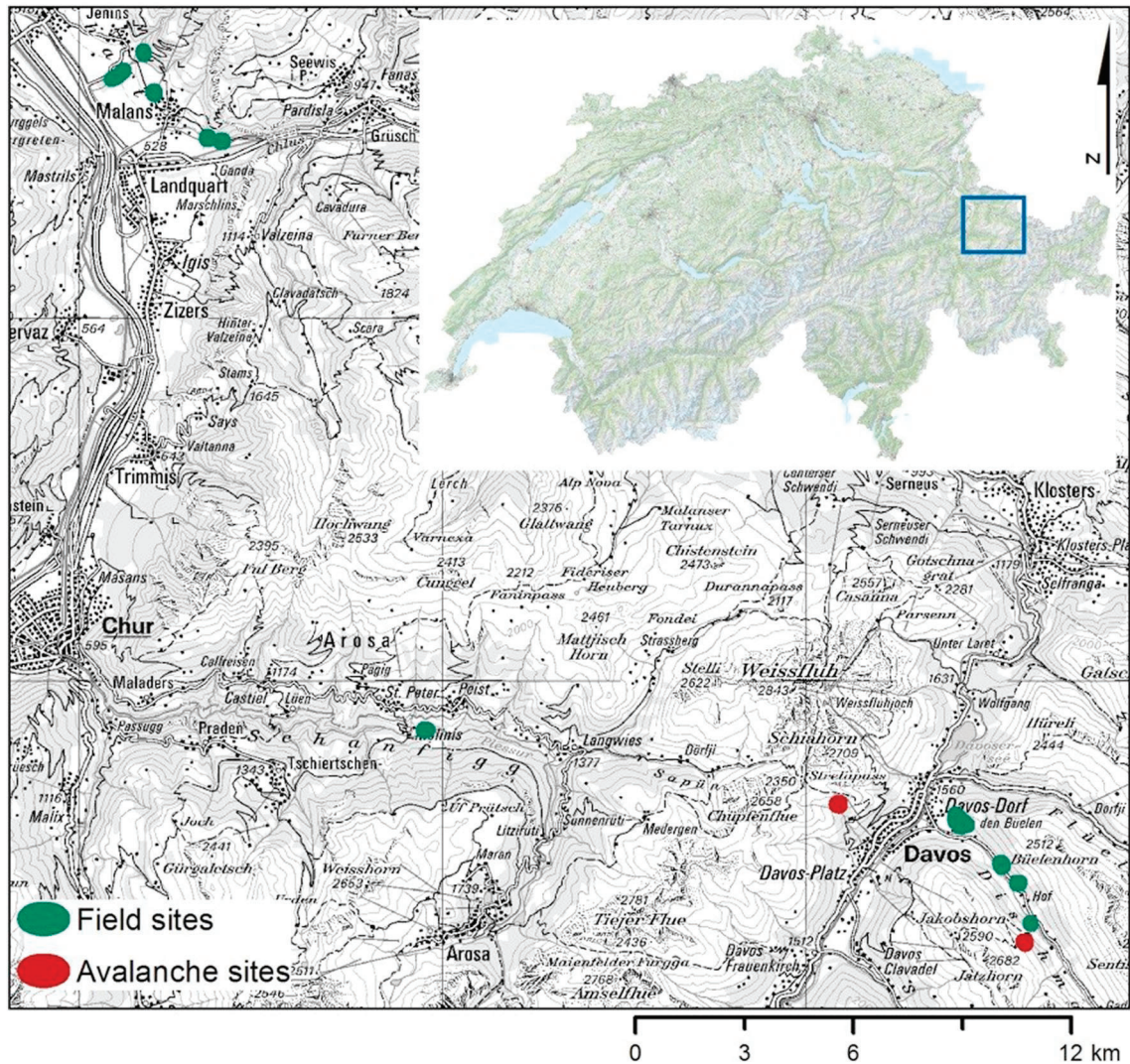
Fig. 1. Location of the avalanche sites and the field sites, where the field observation and measurements were done as a part of the control assessment. On the field sites we compared the remote sensing and control method. Pixmap © 2019 swisstopo (5704000000), reproduced by permission of swisstopo (JA100118).

Table 1
Differences between the two models used (VHM$_L$ and VHM$_P$).

	VHM$_L$	VHM$_P$
Origin of DSM	LiDAR	stereo images
Time of acquisition	2015	2011–2012
Instrument	laser scanner RiEGL LMS-Q 780	sensor Leica ADS80
Resolution	1 m (resampled from 0.5 m)	1 m (resampled from 2 m)

field). For the categorical data (surface roughness categories: 1-smooth, 2-knobby and 3-rough) within the plots, a confusion matrix technique was applied to compare the field observations and DTM derived surface roughness. The field measurements of single roughness elements were compared to mean and median values of DTM derived roughness.

2.3. Avalanche case studies

Two forest avalanches from the winter 2007/2008 and 2017/2018 were chosen to test the forest parameters estimated by remote sensing methods. To represent the forest avalanche interaction with the RAMMS software (Christen et al., 2010), forested areas were identified and corresponding values for input parameters (tree species, diameter at breast

height (DBH) and detrainment coefficient K) were assigned according to the control and remote sensing methods. K-values represent the capacity to detrain snow behind trees and tree groups as the avalanche moves through the forest. The detrainment of avalanche snow removes momentum from the flow, effectively decelerating the avalanche (Feistl et al., 2014). The K-values are classified by tree type, crown coverage and surface roughness according to the look-up table, which is based on avalanche-forest interaction case studies (Feistl et al., 2014; Teich et al., 2013a; Feistl, 2015; see Table 2). The DBH was measured in the field (control method) and calculated using an exponential function with the height extracted from the remote sensing methods. In the simulation model, the information on DBH together with tree species defines the tree breakage threshold (Feistl et al., 2014).

The first avalanche track of the Schatzalp avalanche is located in the main valley above the town Davos (Switzerland); the Teufi avalanche track is situated on the orographic left side of Dischma, SE lateral valley stretching from Davos (Fig. 1). The Schatzalp avalanche had a release area above the treeline, the Teufi avalanche within the forest, and both had runout zones within forest cover. These study cases may represent good examples of the stopping of an avalanche flow, because the snow detrainment effects within the forest could be approximated. To test the influence of the forest parameters assessed by different methods on the avalanche simulation, a set of avalanche parameters (Table 3) were

Table 2

Forest parameters determining the detrainment coefficient K, which enters the avalanche simulation in RAMMS. Amended from RAMMS "Look-up table of K-values for forest shape files" (Feistl, 2015).

Forest type	Crown coverage	Surface roughness	K-value
Evergreen/mixed	Dense (> 70%) coverage	Rough; height > 100 cm	48
		Knobby; height 20–100 cm	38
		Smooth; height < 20 cm	28
	Scattered (40% - 70%) coverage	Rough; height > 100 cm	43
		Knobby; height 20–100 cm	33
		Smooth; height < 20 cm	23
	Open (20% - 40%) coverage	Rough; height > 100 cm	38
		Knobby; height 20–100 cm	28
		Smooth; height < 20 cm	18
Larch/deciduous trees	Dense (> 70%) coverage	Rough; height > 100 cm	35
		Knobby; height 20–100 cm	25
		Smooth; height < 20 cm	15
	Scattered (40% - 70%) coverage	Rough; height > 100 cm	30
		Knobby; height 20–100 cm	20
		Smooth; height < 20 cm	10
	Open (20% - 40%) coverage	Rough; height > 100 cm	25
		Knobby; height 20–100 cm	15
		Smooth; height < 20 cm	5

Table 3

Parameters used for back calculation of Teufi and Schatzalp avalanches.

	Parameter	Unit	Symbol	Schatzalp	Teufi
Release	*Height*	m	d_0	0.5	0.5
	Density	kg/m³	ρ_0	200	350
	Temperature	°C	T_0	−7	−2
	Water content	%	w_0	0	0
Erodible snow cover	*Height*	m	d_Σ	0.5	0.5
	Density	kg/m³	ρ_Σ	175	400
	Temperature	°C	T_Σ	−7	0
	Water content	%	w_Σ	0	5

defined to fit the runout of an observed avalanche. The simulation outputs were compared to the control method (using field estimated forest structure). The release areas for these avalanches were defined according to the topography and crosschecked with the observed release areas.

In order to evaluate the influence of forest parameters on the avalanche simulation results, we investigated: the spatial maxima of the i) peak flow depth, ii) peak (depth averaged) flow velocity, as well as iii) the runout determined as projected run length in the main flow direction along the avalanche. Herein peak refers to the maximum over the simulation duration and the maximum to the spatial maximum over the entire simulation domain. The runout is determined manually, where the peak flow depth drops to zero. This approach appears sufficient due to the little number of simulations, otherwise in the case of e.g. large scale hazard mapping, more automatized methods to evaluate runout may be required (Fischer, 2013; Teich et al., 2013a).

2.3.1. Schatzalp avalanche

The Schatzalp avalanche (Fig. 2, on the left) released above the local treeline at an elevation of 2110 m a.s.l. on 22 January 2018. The avalanche was released from three separate gullies on a 36–40° steep and SE-S-exposed slope. It merged subsequently to one avalanche and travelled through forested terrain until an elevation of 1830 m a.s.l. The cause for this avalanche was an additional loading from new snow onto the existing snowpack, which triggered several dry-snow slab avalanches in the region of Davos. The Schatzalp avalanche was a medium sized (< 10,000 m³; EAWS, 2012) avalanche with the total length of 630 m. The forest in this avalanche track is characterized by pine trees (*Pinus cembra*) close to the treeline and spruce trees (*Picea abies*) in the lower parts.

2.3.2. Teufi avalanche

The wet snow avalanche Teufi (Fig. 2, on the right) released from the slope of approximately 40° at 2080 m a.s.l. due to a rain-on-snow

event in the night from 22nd to 23rd of April 2008. This avalanche flowed to the valley bottom at 1690 m a.s.l. The Teufi avalanche was a small to medium sized (1000–10,000 m³; EAWS, 2012) avalanche with the total length of 400 m and 390 m of fall height. The forest is dominated by pine (*Pinus cembra*) in the upper part, green alder (*Alnus viridis* subsp. *viridis*) within the avalanche track, and spruce (*Picea abies*) and larch (*Larix decidua*) in the lower part of the avalanche track.

2.3.2.1. Avalanche simulation with varying forest cover. The Teufi avalanche served also as case study to investigate effects of forest structure, defined by remote sensing methods, on the model parameters and the simulated runout distance (research topic 3). Two different remote sensing methods (VHM_L and VHM_P) and a control method were used to estimate the forest in the release area of the Teufi avalanche study case. The avalanche was simulated using parameters to fit an actual wet snow avalanche from 2008. We aimed not to evaluate simulation results with field observation, but to investigate the effect of forest in the release area and the change of the forest cover within the avalanche track. Therefore the size of the release area was defined through digital data on topography and forest cover, and not by the field observation. The avalanche was simulated also with different forest structures at the lower part of the avalanche track: before and after the forest destruction in order to see the differences the forest change has on the runout distance. The forest structure for RAMMS simulation (K-values) was estimated using orthophotos before and after the avalanche events in combination with the local forest inventory documentation.

3. Results

3.1. Forest parameters determined by remote sensing methods

3.1.1. Tree heights

Observed or predicted distributions of tree heights on the plots were similar for the field measurements as well as for the remote sensing methods (Fig. 3, Table 4). Counting for all plots together, remote sensing methods estimated mean tree heights well (mean absolute error of the estimated heights from VHM_L was 2.8 m and from VHM_P it was 3.2 m) and there was no significant difference between the methods (Analysis of variance: ANOVA, $p = .53$). The differences in mean tree height by forest type between methods were not significant for deciduous forest type as determined by the ANOVA ($p = .90$). However, there was a significant difference (ANOVA, $p = .02$) in the evergreen forest type between the VHM_L and VHM_P (Tukey test). Minimum and maximum tree heights in evergreen forest type were noticeably smaller

Fig. 2. Schatzalp avalanche (on the left; photo SLF) and Teufi avalanche (on the right; photo Peter Bebi). Schatzalp avalanche represents a good example of a dry snow slab avalanche, the Teufi avalanche of a wet snow avalanche.

in the VHM$_P$, while the field measured minimum tree heights and minimum tree heights extracted from VHM$_L$ were similar. Maximum heights were larger in the VHM$_L$ estimates for the evergreen forest type compared to the VHM$_P$, but with no difference in comparison to the control method (field measurements). In the deciduous forest type minimum and maximum tree heights were similar across the methods.

The results of tree height vertical agreement assessment of the remote sensing methods (VHM$_P$ and VHM$_L$) conducted in 107 plots are shown in the Table 4. VHM$_L$ showed higher accuracy in all measures, i.e. higher agreement with the tree heights measured in the field than VHM$_P$ (e.g. robust estimator of the standard deviation was 2.71 m for VHM$_L$ and 3.37 m for VHM$_P$).

There was a high correlation between the field measured tree heights and the VHM$_L$ obtained heights (Pearson's $r = 0.92$) as well as the field measurements to the VHM$_P$ heights (Pearson's $r = 0.89$). Looking at the deciduous and evergreen groups separately, the deciduous group VHM$_P$ (Pearson's $r = 0.91$) performed better than VHM$_L$ (Pearson's $r = 0.88$), but in the evergreen group VHM$_L$ (Pearson's $r = 0.83$) fitted better with the control heights in comparison to VHM$_P$ (Pearson's $r = 0.72$).
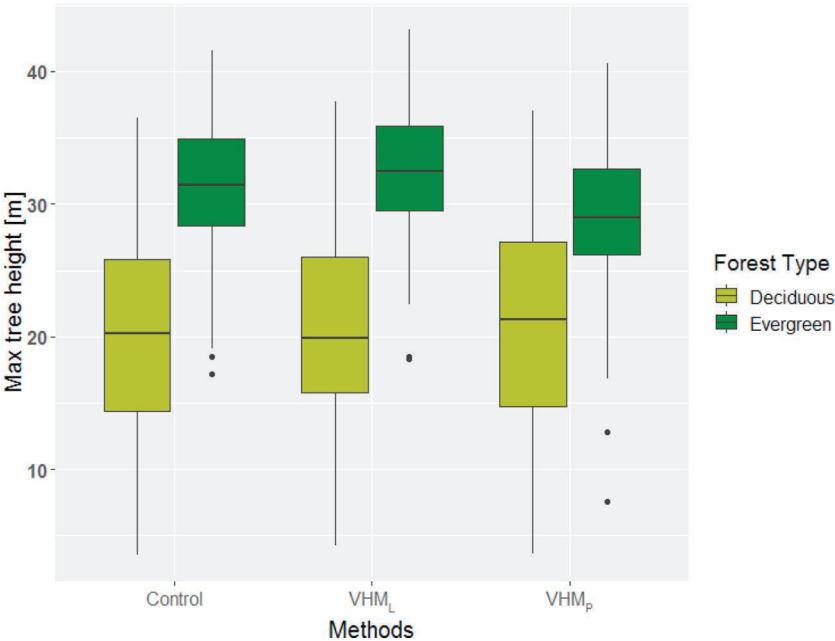
Table 4

The accuracy assessment of the differences in heights measured in the field and extracted by remote sensing methods (VHM$_L$ and VHM$_P$).

Accuracy measure	Control - VHM$_L$			Control - VHM$_P$		
	All	Deciduous	Evergreen	All	Deciduous	Evergreen
Median [m]	−1.17	−0.9	−1.3	0.53	−0.68	1.33
NMAD [m]	2.71	3.17	2.23	3.37	3.17	2.57
68.3% quantile [m]	1.22	0.56	−0.21	1.72	0.73	2.73
95% quantile [m]	5.11	5.5	2.69	7.8	5.69	10.82

NMAD – normalized median absolute deviation.

3.1.2. Crown coverage

The agreement between remote sensing based crown coverage assessment and the control method differed according to crown coverage class and forest type (Table 5, Fig. 4). The best agreement was found for dense (crown coverage > 70%) and deciduous forests while crown coverage of dense and evergreen forests ($\tilde{x} = 100$) was overestimated

Fig. 3. Tree height measured with different methods (in the field using Vertex as control method, and derived from the models based on LiDAR and photogrammetric DSM). The VHM$_L$ provides estimates with smallest differences to control method in both forest types (deciduous and evergreen) and overestimates the heights. The VHM$_P$ overestimates heights in the deciduous forest type and underestimates heights in the evergreen forest type.

Table 5
Median value of crown coverage for different measuring methods (control, VHM_L and VHM_P) by forest type (deciduous and evergreen) and crown coverage class (open: 20%–40%, scattered: 40%–70% and dense: > 70%).

Method	Deciduous			Evergreen		
	Open	Scattered	Dense	Open	Scattered	Dense
Control	35	50	100	30	60	90
LiDAR	35	70	100	40	65	90
Photogrammetry	30	60	100	20	55	100

with VHM_P compared to VHM_L or the control method (both $\tilde{x} = 90$). In deciduous forests with scattered crown coverage, both models overestimated the observation ($\tilde{x}_C = 50$, $\tilde{x}_P = 60$, $\tilde{x}_L = 70$), while in evergreen forests of the same forest cover class, VHM_P slightly underestimated ($\tilde{x}_P = 55$) and VHM_L slightly overestimated ($\tilde{x}_L = 65$) the observations ($\tilde{x}_C = 60$). Open forests were again better estimated in the deciduous forest type, with little underestimation in VHM_P ($\tilde{x}_C = 35$, $\tilde{x}_P = 35$, $\tilde{x}_L = 30$). In the open class evergreen forest type, crown coverage is overestimated by the VHM_L ($\tilde{x}_L = 40$) and underestimated by the VHM_P ($\tilde{x}_P = 20$) compared to control method ($\tilde{x}_C = 30$). We found no significant difference between the models and control method (ANOVA, $p = .11$ for open, $p = .42$ for scattered and $p = .11$ for dense).

3.1.3. Terrain roughness

The assessment of surface roughness based on DTM (1 m resolution) differed according to roughness category (Fig. 6). Roughness determined by the DTM showed a high correspondence to the control method in the smooth category. However, the estimation of the knobby and rough categories was limited, since the DTM underestimated the roughness. There was no significant difference comparing the 5 m and 10 m radius roughness observed in the field and the roughness derived from DTM (Standard t-test). The 5 m radius surface roughness was well estimated by the roughness derived from DTM in the smooth category, 47 plots (80%; Fig. 6). Categories knobby and rough were mostly underestimated by the remote sensing method (35% classified as knobby and 22% as rough). The roughness at the 10 m buffer was as well underestimated for the two higher roughness categories (knobby and rough). The roughness category smooth was well represented with 39 plots matching with the classification (71%; Fig. 6).

Single roughness elements (stones, tree stumps) measured in the field could generally not be identified by increased roughness values derived from DTM. Some of them are optically visible in the map

(Fig. 7), but most of them are not detectable with the roughness derived from DTM.

3.2. Avalanche case studies

3.2.1. Schatzalp avalanche

The forest was classified differently by the remote sensing methods in comparison to the control method. The largest difference occurred in the estimation of forest cover by the VHM_P, where some of the vegetation in the upper part of an avalanche track was not detected.

The simulated avalanche followed a very similar path and showed similar flow heights when using parameters determined by the different remote sensing methods, but runout distance varied according to the applied remote sensing method (Fig. 8). Runout distance of Schatzalp avalanche and the peak flow velocity (18.1 m/s) did not differ from the control method using VHM_L to determine the forest parameters (Fig. 8, A). However, runout distance of the avalanche was 42 m longer when using the VHM_P and the peak flow velocity increased by 4.4 m/s when using the VHM_P instead of the control method (Fig. 8, B).

3.2.2. Teufi avalanche

The forest in the avalanche track of Teufi was detected well using both remote sensing methods although different roughness estimation produced some differences in K-values. Both remote sensing methods underestimated the K-values in the lower part, but overestimated it in the upper part of the avalanche track compared to the control method.

Simulation of the avalanche assessed by the control and remote sensing methods revealed similar outputs (Fig. 9). The peak flow velocity was slightly lower with the VHM_L ($Vmax_L = 20.0$ m/s) compared to the simulation with the VHM_P ($Vmax_P = 22.5$ m/s) and the control method ($Vmax_C = 24.2$ m/s). However, runout distances were almost identical with some small deviation when using VHM_P (3 m longer runout distance, with respect to the flow depth equal to zero, compared to the control method, Fig. 9).

3.3. Avalanche simulation with varying forest cover

The smallest release area of the Teufi avalanche was estimated using the VHM_L (2535 m^2) method, due to denser estimated forest cover in that area. VHM_P did not detect some of the vegetation in comparison to VHM_L. This resulted in a larger release area (3313 m^2). Using the control method, green alder (*Alnus viridis* subsp. *viridis*) was distinguished from the other vegetation and was included in the release
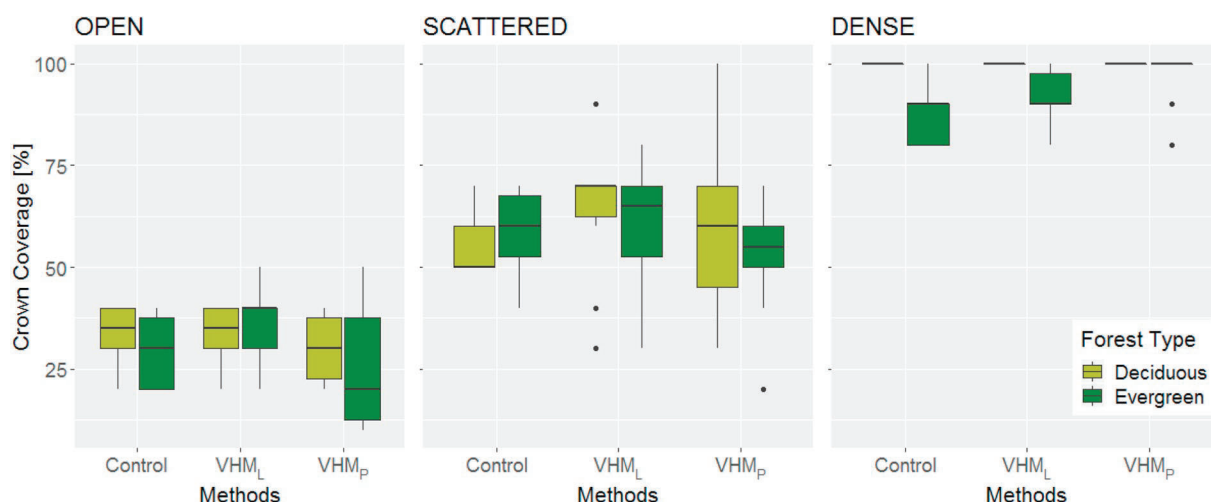
Fig. 4. Distribution of crown coverage by forest type (deciduous and evergreen) and method in plots with crown coverage classes: open (20%–40%), scattered (40%–70%) and dense (> 70%). The thick lines represent the medians while the bottom and top boundaries of the box show 25th and 75th percentiles, respectively. The crown coverage estimates from remote sensing methods (VHM_L and VHM_P) correspond to the crown coverage defined by control method.

area. This flexible shrub is often bent under the snow cover, resulting in a larger release area of 4488 m^2. Simulation of the avalanche with the largest release area caused the longest avalanche runout distance (472 m in comparison to 464 m and 455 m for orthophoto, VHM$_P$ and VHM$_L$, respectively).

After the avalanche in 2008 (Fig. 2) and a secondary avalanche in 2009, a part of the forest in the avalanche track was destroyed (Fig. 10). Simulating the Teufi avalanche with the same parameters (Table 3), but with the state of forest cover after 2009 (as seen in the Fig. 10), resulted in a longer runout distance (60 m longer, Fig. 11).

4. Discussion

4.1. Forest parameters determined by remote sensing methods

Tree heights were well estimated by the LiDAR and photogrammetry methods. Although there was no significant difference between the methods when considering all the plots together (evergreen and deciduous); tree heights were higher when estimated with the LiDAR method compared to the photogrammetry method in the evergreen forest type. System errors may occur in both applied methods: the LiDAR method may fail when different objects than those of interest are reflected (Thiel and Schmullius, 2016). In the photogrammetry method the system errors have been mainly related to the structure and texture of the images on northern slopes, where detection of forest is hindered by the shadow (Ginzler and Hobi, 2015). In our analysis, some of the plots were situated on steep mountain sides, where calculation of the vegetation height model using photogrammetry can be problematic (Ginzler and Hobi, 2015). In some cases LiDAR performed better, but we found no evidence for either method being superior in regards to error. The magnitude of errors is comparable to that observed in other studies (Lisein et al., 2013; Gašparović et al., 2017; Fankhauser et al., 2018).

Crown coverage was generally well estimated by both of the models (VHM$_L$ and VHM$_P$). The VHM$_L$ was more accurate than the VHM$_P$ and in some cases overestimated the crown coverage (Fig. 5). The mean model estimations of the crown coverage (under- or overestimated) were always within the crown coverage classification: open (20%–40%), scattered (40%–70%) and dense (> 70%). Such performance allows us to use these models for determination of forest parameters for avalanche simulation. However, as seen in the simulation with varying forest cover, the coverage has an important effect on simulated runout of an avalanche. The LiDAR method is often clearly better for estimating the crown coverage in release areas and should be therefore preferred over the photogrammetry method. The topographical maps are not recommended for forest cover estimation as it was observed that these maps were not always up-to-date. The most precise forest cover and crown coverage is obtained from an orthophoto and therefore its use for forest cover and crown coverage estimation in smaller areas is recommended. We assessed the crown coverage only from summer data,

but the crown coverage of deciduous broadleaved and coniferous forests differs in winter. The different crown coverage in deciduous and evergreen forests has an effect on avalanche formation due to different snow interception (Schneebeli and Bebi, 2004; McClung and Schaerer, 2006; Bebi et al., 2009) and also on avalanche dynamics due to different loading (Feistl et al., 2015). A loading width is smaller, if the trees are leafless or if they are in a dense forest stand (Feistl et al., 2015). These differences are considered by different K-values. One of the forest parameters defining the K-value is the forest type, which is divided to evergreen/mixed and deciduous (Table 2). This classification allows accounting for different effects of deciduous trees as in broadleaved and larch forests (Teich et al., 2013a; Feistl, 2015).

Surface roughness within the studied plots was classified smoother using the DTM (with 1 m resolution), than observed in the field. The single roughness elements (as stones and tree stumps) were mostly not classified by the surface roughness derived from the DTM. However, some of these elements were still visible on the DTM roughness classification. Reasons for local surface roughness smoothing are errors during filtering and interpolation procedures during post-processes of raw data (Höhle and Höhle, 2009). Because already small-scale topographic roughness may have an influence on avalanche flow, surface smoothening may influence runout distance particularly for wet-snow avalanches (Sovilla et al. 2012). In spite of still existing limits to detect surface roughness, we suggest that further attempts to optimise post-processing of high resolution LiDAR-data and further ground-truthing on larger plots may still be valuable in order to further improve the implementation of surface roughness in avalanche simulations.

4.2. Avalanche case studies

The remote sensing methods were tested on the dry-snow avalanche Schatzalp from 2018 and wet-snow avalanche Teufi from 2008 based on the determined forest information. Field data on tree heights and surface roughness, and crown coverage assessment from orthophoto served as control method.

In the case of the Schatzalp avalanche, forest cover determined through different remote sensing methods was not represented equally as by the control method. In the upper part of the avalanche track, VHM$_P$ failed to detect some of the forest, which had an influence on the simulated runout distance. As a consequence, the simulated runout distance of the Schatzalp avalanche was too long when using VHM$_P$, which underestimated the forest cover. The simulated runout distance was well represented using the VHM$_L$ to determine forest parameters in comparison to the simulation using control method that represents the observation. LiDAR based vegetation height model (VHM$_L$) delivered thus in the case of Schatzalp avalanche more similar results to the control method than the model based on photogrammetry (VHM$_P$). Forest cover in the avalanche track of Teufi was represented comparatively well by the remote sensing methods. Some differences
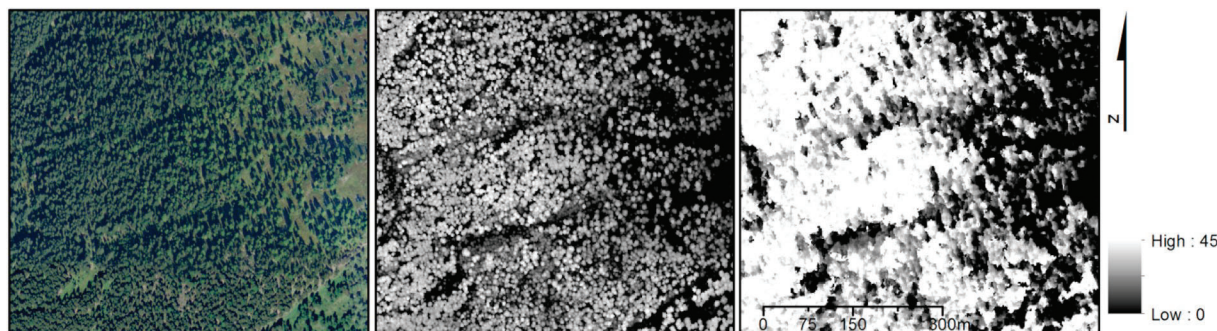

Fig. 5. Visual comparison between the control assessment via orthophoto and vegetation height models (orthophoto on the left, VHM$_L$ in the middle and VHM$_P$ on the right) in the conifer forest. Using VHM$_L$ single trees are detectable in comparison to the VHM$_P$, where smoothing does not allow a direct identification. However, the forest gaps are identifiable from all methods. Orthoimagery © 2019 swisstopo (5704000000), reproduced by permission of swisstopo (JA100118).
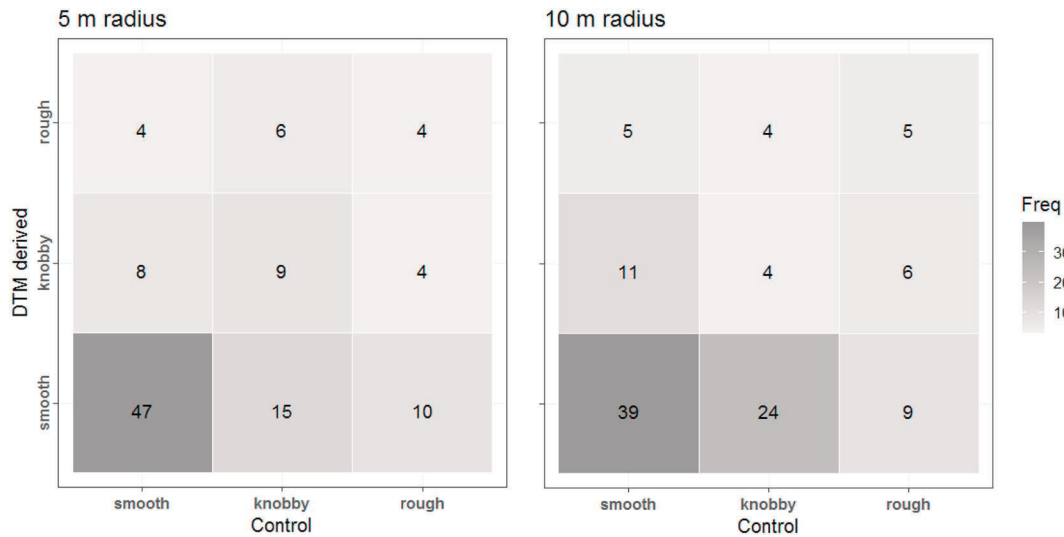
Fig. 6. Confusion matrix for the roughness observation in the field compared to the roughness derived from the DTM. Two radii were used to compare the surface roughness (5 m on the left, 10 m on the right). The best predictions are in the category smooth for both radii (80% for the 5 m buffer and 71% for the 10 m buffer).

occurred in the K-value, where the VHM$_P$ showed higher crown coverage than estimated from the orthophoto or from the VHM$_L$. However, these differences did not influence the simulated avalanche runout.

The two case studies suggest that the usage of LiDAR data for the determination of forest parameters and their implementation in avalanche simulation models is recommended if they are available. This is particular true for large-scale hazard applications where photogrammetric data may not deliver a homogenous VHM-quality compared to LiDAR-data and where field-verifications are time-consuming. Photogrammetric data may however also deliver feasible simulation outputs, in particular if they are combined with field observation and orthophoto in order to carefully classify forest structure. It has also been shown, that further improvement of remote sensing data and their usage for determination of forest for avalanche simulation do not necessarily lead to a better estimation of

avalanche runout, since the uncertainties related to the better process understanding remain often high (Stritih et al., 2019). Better identification and estimation of release areas reduces significantly the uncertainty in avalanche simulation (Bühler et al., 2018). Satellite, airborne and Un-manned Aerial System (UAS) based remote sensing can in the future help to improve the accurate and timely mapping of avalanche release areas, substantially improving their understanding and modeling (Bühler et al., 2009; Lato et al., 2012; Bühler et al., 2016; Eckerstorfer et al., 2016; Korzeniowska et al., 2017; Bühler et al., 2019).

4.3. Avalanche simulation with varying forest cover

The Teufi avalanche was simulated with two different forest structures (before and after the avalanches) and the runout of the simulated
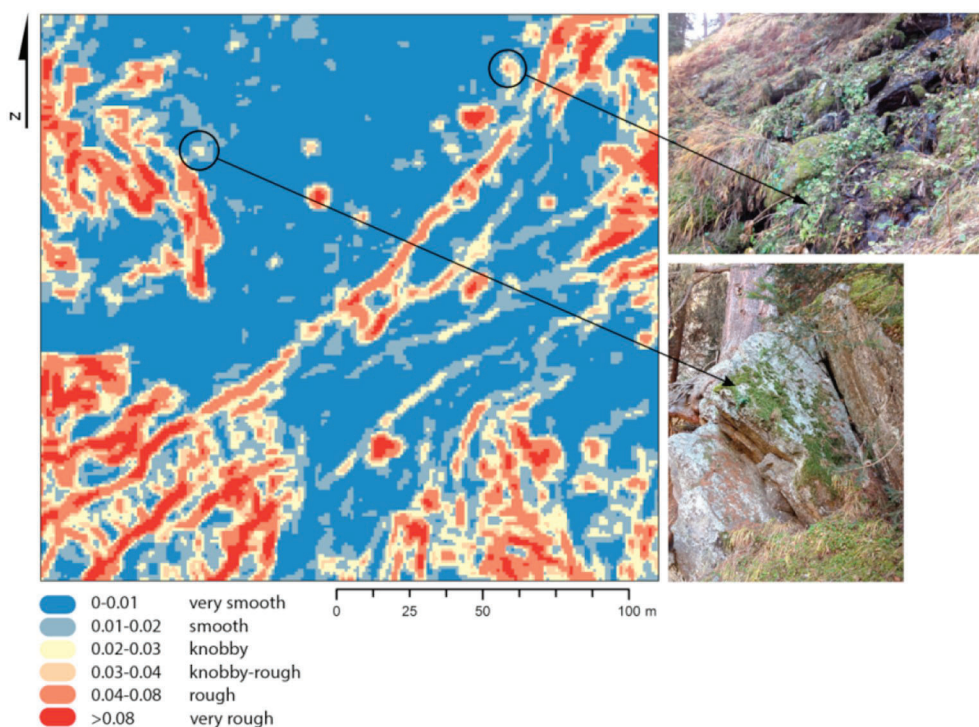

Fig. 7. Roughness classification derived from DTM in the area of interest with two examples of surface roughness elements.
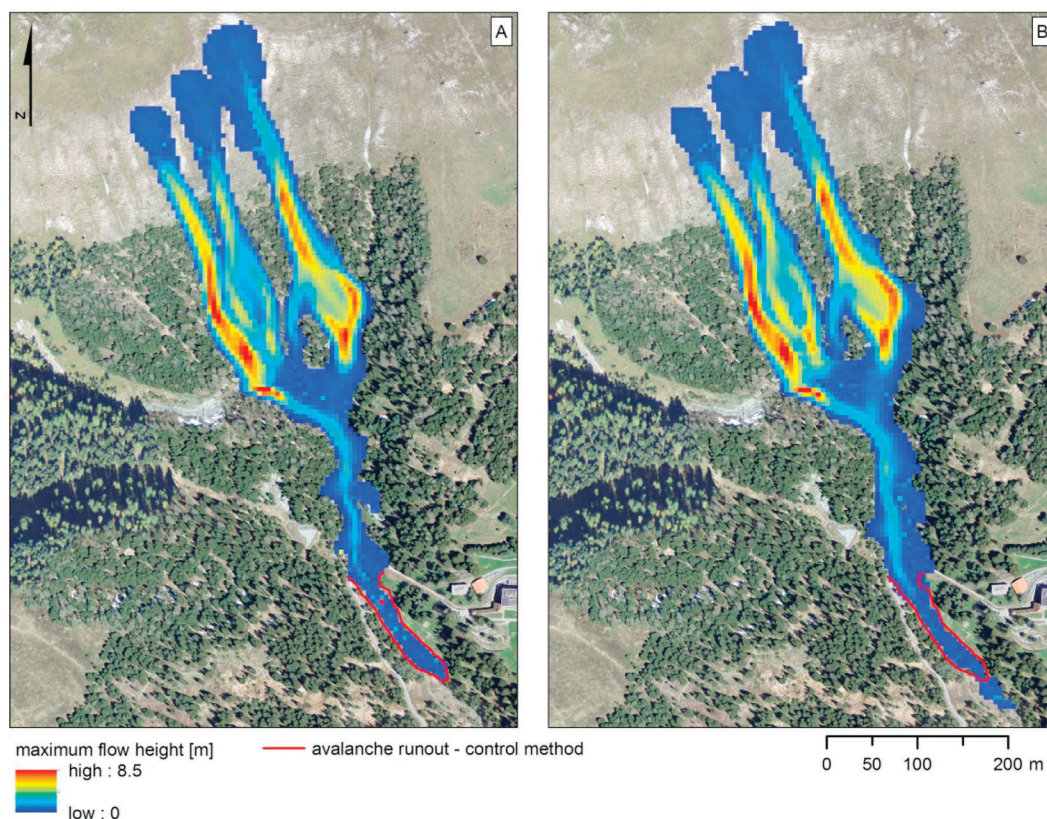
Fig. 8. Simulated maximum flow height of the Schatzalp avalanche using two different remote sensing methods (VHM$_L$ (A) and VHM$_P$ (B)). The runout distance of the control method, corresponding to the field observations, where the deposition height transitions to zero is represented by the red line. The maximum flow height values are similar for both methods. Longer runout distance (about 42 m longer) occurs when using the photogrammetry method to determine the forest parameters in comparison to the parameters defined in the field. The differences between the peak flow heights from simulations using different methods were negligible (8.7 m for VHM$_L$ and 8.6 for both the control method as well as for VHM$_P$). Orthoimagery © 2019 swisstopo (5704000000), reproduced by permission of swisstopo (JA100118). (For interpretation of the references to colour in this figure legend, the reader is referred to the web version of this article.)

avalanche results in shorter distance before the forest destruction. The most common impacts on avalanche activity were lower tree age and size, higher share of deciduous species, higher shrub and herbal cover (Vacchiano et al., 2015).

As in the case of the avalanche track at Teufi, the forest structure and composition changed after the forest destruction due to the avalanches from young spruce dominating forest towards green alder dominated forest. Shrubs as green alder or dwarf pine are very common in the release areas, but also in the avalanche track. However, the impact of green alder on avalanche formation and dynamics is still not clear and may differ according to avalanche size. Some authors state a negative effect, as that suppressed branches of green alder create gliding surface for avalanches (Aley, 1960; Hug, 2013). Also green alder does not offer the same protection function as mountain forests, which cannot be regained, since green alder hinders forest succession (Bühlmann et al., 2014). On the other hand, some authors report positive effects of green
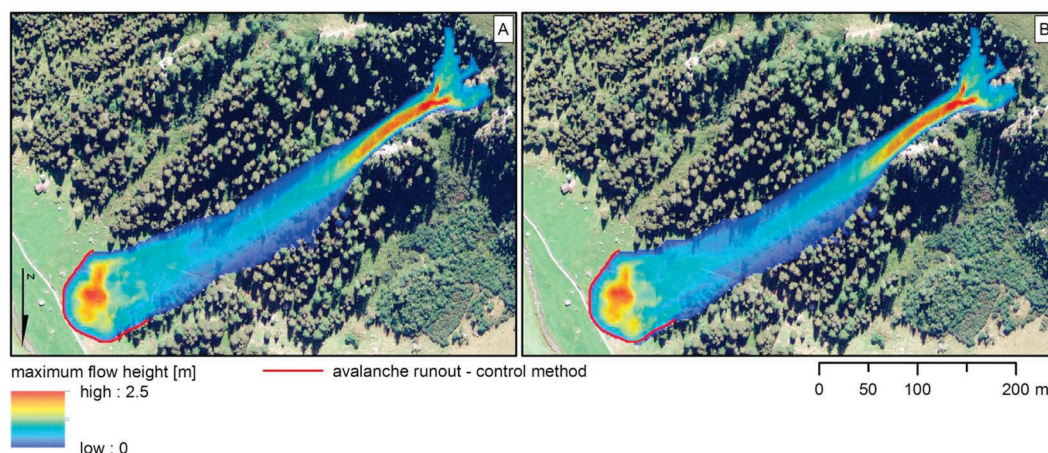

Fig. 9. Comparison between simulated maximum flow height of Teufi avalanche using two different remote sensing methods (VHM$_L$ (A) and VHM$_P$ (B)) and the reference simulation runout obtained by parameters defined through the control method. The differences were negligible in the peak flow height (2.2 m and 2.3 m for VHM$_L$ and VHM$_P$, respectively) and the runout distance (± 3 m). Orthoimagery © 2019 swisstopo (5704000000), reproduced by permission of swisstopo (JA100118).
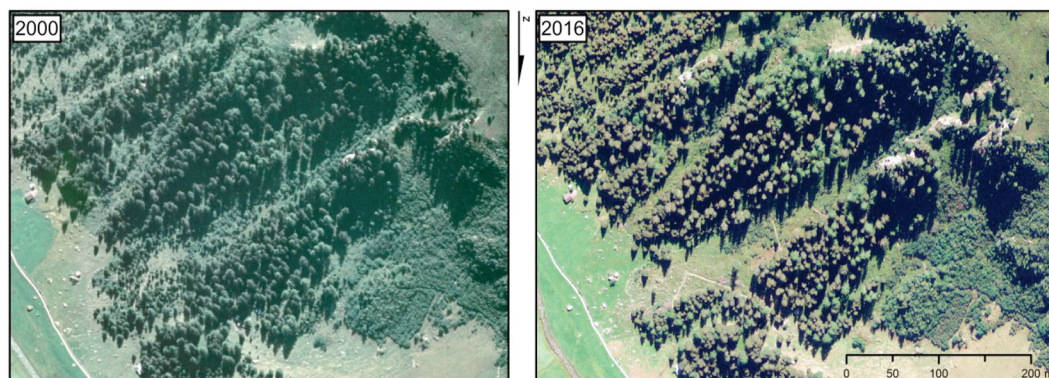
Fig. 10. Forest in the avalanche track before (on the left, year 2000) and after (on the right, year 2016) the forest destruction. Orthoimagery © 2019 swisstopo (5704000000), reproduced by permission of swisstopo (JA100118).
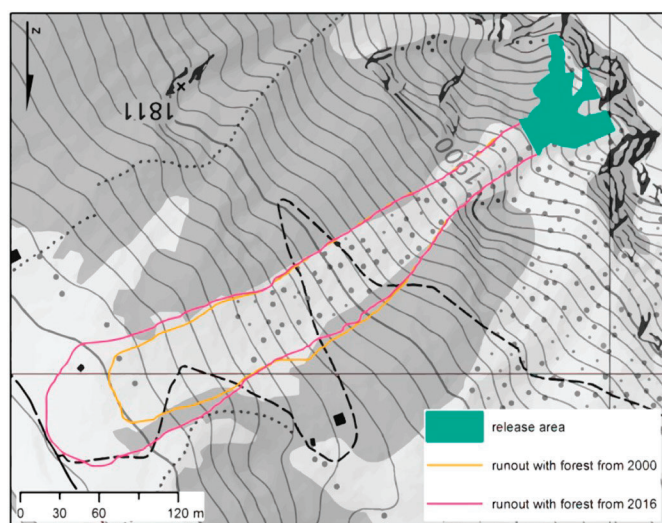

Fig. 11. Runout distance of the same avalanche using different forest structures, before and after the forest destruction. After the forest destruction, the runout of the avalanche results in longer distance of about 60 m. Pixmap © 2019 swisstopo (5704000000), reproduced by permission of swisstopo (JA100118).

alder on the stabilizing of snowpack by increasing the surface roughness and therefore the basal friction, even though the green alder is often buried under the snow (Poncet, 2004). Our result suggests that for avalanches like our example of the Teufi avalanche, green alder increases the surface roughness in the avalanche track.

Less forest cover leads to less forest detrainment and longer runout distance. When avalanche disturbance is frequent or substantial, a forest is unable to establish and create essential protection. It is then unable to establish or it is constantly disturbed in an early successional stage (Johnson, 1987). Although both investigated remote sensing methods led to similar forest parameters, and therefore also similar K-values for the avalanche simulation, our comparison showed that remote sensing methods were in particular useful to evaluate effects of changes in forest cover and that an avalanche event may strongly increase the intensity of the next event. In such cases of compounded disturbances, the protection function is lowered against future avalanches and may also be less effective against rockfall or other natural hazards (Vacchiano et al., 2015). After forest damage within the avalanche track, future events should therefore be expected to have larger impacts and longer runout distances.

5. Conclusions

Remote sensing data with a resolution of 1 m are generally suitable to determine relevant forest parameters for avalanche simulation

models. Tree heights are well estimated by both tested remote sensing methods and the analysis is incomparably faster than measuring trees in the field. Crown coverage is however best estimated visually on the basis of orthophotos or hillshades of the LiDAR-based VHM compared to a photogrammetric-based VHM, and surface roughness is underestimated using a 1 m resolution DTM. In order to obtain more precise model inputs, it is recommended to use a combination of different methods to generate forest data and to test higher DTM resolution for the estimation of surface roughness.

The simulation outputs (using the forest information from both of the remote sensing methods) have shown to be sufficiently accurate for numerical modeling, as well as real applications in avalanche hazard mapping. However, an underestimation of forest cover, in particular in or near avalanche release areas, can lead to an overestimation of runout distance in avalanche simulations. Future research should therefore focus on the precise estimation of forest cover in release areas and on effects of forest cover changes on avalanche runout.

Spatial variations and temporal changes in forest cover and forest structure may substantially influence the runout distance of small to medium size avalanches and should be taken into account in avalanche modeling. Such variations of the forest cover can be easily assessed using remote sensing methods, as they are becoming increasingly available in higher resolution at any time needed.

Declaration of Competing Interest

The authors declare that they have no known competing financial interests or personal relationships that could have appeared to influence the work reported in this paper.

References

Aley, T.J., 1960. Snow Avalanche Tracks and their Vegetation. Master thesis. University of California (52 p).
Bebi, P., Kienast, F., Schönenberger, W., 2001. Assessing structures in mountain forests as a basis for investigating the forests' dynamics and protective function. For. Ecol. Manag. 145, 3–14.
Bebi, P., Kulakowski, D., Rixen, C., 2009. Snow avalanche disturbances in forest ecosystems - State of research and implications for management. For. Ecol. Manag. 257

(9), 1883–1892.

Bühler, Y., Hüni, A., Christen, M., Meister, R., Kellenberger, T., 2009. Automated detection and mapping of avalanche deposits using airborne optical remote sensing data. Cold Reg. Sci. Technol. 57, 99–106.

Bühler, Y., Adams, M.S., Bösch, R., Stoffel, A., 2016. Mapping snow depth in alpine terrain with unmanned aerial systems (UASs): potential and limitations. Cryosphere 10, 1075–1088.

Bühler, Y., von Rickenbach, D., Stoffel, A., Margreth, S., Stoffel, L., Christen, M., 2018. Automated snow avalanche release area delineation – validation of existing algorithms and proposition of a new object-based approach for large scale hazard indication mapping. Nat. Hazards Earth Syst. Sci. 18, 3235–3251.

Bühler, Y., Hafner, E.D., Zweifel, B., Zesiger, M., Heisig, H., 2019. Where are the avalanches? Rapid mapping of a large snow avalanche period with optical satellites. The Cryosphere Discuss. https://doi.org/10.5194/tc-2019-119. (in review).

Bühlmann, T., Hiltbrunner, E., Körner, C., 2014. Alnus viridis expansion contributes to excess reactive nitrogen release, reduces biodiversity and constrains forest succession in the Alps. Alp Botany 124, 187–191.

Christen, M., Kowalski, J., Bartelt, P., 2010. RAMMS: Numerical simulation of dense snow avalanches in three-dimensional terrain. Cold Reg. Sci. Technol. 63 (1–2), 1–14.

EAWS, 2012. European avalanche size classification. 2013a In: Teich, M., Fischer, J.-T., Feistl, T., Bebi, P., Christen, M., Grêt-Regamey, A. (Eds.), Computational Snow Avalanche Simulation in Forested Terrain. Natural Hazards and Earth System Science, vol. 14(8). pp. 2233–2248.

Eckerstorfer, M., Bühler, Y., Frauenfelder, R., Malnes, E., 2016. Remote sensing of snow avalanches: recent advances, potential, and limitations. Cold Reg. Sci. Technol. 121, 126–140.

Fankhauser, K.E., Strigul, N.S., Gatziolis, D., 2018. Augmentation of traditional forest inventory and airborne laser scanning with unmanned aerial systems and photogrammetry for forest monitoring. Remote Sens. 10 (10), 1562.

Feistl, T., 2015. Vegetation Effects on Avalanche Dynamics. Dissertation. Technische Universität München, Ingenieurfakultät Bau Geo Umwelt.

Feistl, T., Bebi, P., Teich, M., Bühler, Y., Christen, M., Thuro, K., Bartelt, P., 2014. Observations and modeling of the braking effect of forests on small and medium avalanches. J. Glaciol. 60 (219), 124–138.

Feistl, T., Bebi, P., Christen, M., Margreth, S., Diefenbach, L., Bartelt, P., 2015. Forest damage and snow avalanche flow regime. Natural Hazards and Earth System Science 15 (6), 1275–1288.

Fischer, J.T., 2013. A novel approach to evaluate and compare computational snow avalanche simulation. Nat. Hazards Earth Syst. Sci. 13, 1655–1667.

Gašparović, M., Seletković, A., Berta, A., Balenović, I., 2017. The Evaluation of Photogrammetry-Based DSM from Low-Cost UAV by LiDAR-Based DSM. South-east European Forestry 8 (2) early view.

Giacona, F., Eckert, N., Mainieri, R., Martin, B., Corona, C., Lopez-Saez, J., Monnet, J.-M., Naaim, M., Stoffel, M., 2018. Avalanche activity and socio-environmental changes leave strong footprints in forested landscapes: A case study in the Vosges medium-high mountain range. Annals of Glaciology 1–23.

Ginzler, C., Hobi, M., 2015. Countrywide stereo-image matching for updating digital surface models in the framework of the Swiss national forest inventory. Remote Sens. 7 (4), 4343–4370.

Höhle, J., Höhle, M., 2009. Accuracy assessment of digital elevation models by means of

robust statistical methods. ISPRS J. Photogramm. Remote Sens. 64, 398–406.

Hug, M., 2013. Überlebenkünstlerin Alpenerle. Bergfwald Projekt: specht 2–4.

Ivosevic, B., Han, Y.-G., Kwon, O., 2017. Calculating coniferous tree coverage using unmanned aerial vehicle photogrammetry. Journal of Ecology and Environment 41, 10.

Johnson, E.A., 1987. The relative importance of snow avalanche disturbance and thinning on canopy plant populations. Ecology 68, 43–53 In: Brang, P., Schönenberger, W., Ott, E., Gardner, B. (Eds.), 2001. 3: Forests as Protection from Natural Hazards. The Forests Handbook. Volume 2. Applying Forest Science for Sustainable Management Wiley-Blackwell In: Evans J., 2001. (816 p).

Korzeniowska, K., Bühler, Y., Marty, M., Korup, O., 2017. Regional snow-avalanche detection using object-based image analysis of near-infrared aerial imagery. Nat. Hazards Earth Syst. Sci. 17, 1823–1836.

Lato, M.J., Frauenfelder, R., Bühler, Y., 2012. Automated Avalanche Deposit Mapping From VHR Optical Imagery, Proceedings, 2012 International Snow Science Workshop, Anchorage, Alaska, 2012. pp. 392–394.

Lisein, J., Pierrot-Deseilligny, M., Bonnet, S., Lejeune, P., 2013. A Photogrammetric Workflow for the creation of a Forest Canopy Height Model from Small Unmanned Aerial System Imagery. Forests 4, 922–944.

McClung, D.M., Schaerer, P., 2006. The Avalanche Handbook, 3rd ed. Mountaineers Books (342 p).

Poncet, A., 2004. A plea in favour of a number of subalpine species that are effective in securing the snow blanket and controlling avalanches. Revue Forestiere Francaise 56 (3), 203–212.

Sappington, J., Longshore, K., Thomson, D., 2007. Quantifying landscape ruggedness for animal habitat analysis: a case study using Bighorn Sheep in the Mojave Desert. J. Wildlife Manage. 71, 1419–1426.

Schneebeli, M., Bebi, P., 2004. Snow and avalanche control. Hydrology 397–402.

Stritih, A., Bebi, P., Grêt-Regamey, A., 2019. Quantifying uncertainties in earth observation-based ecosystem service assessments. Environ. Model. Softw. 111, 300–310.

Takeuchi, Y., Torita, H., Nishimura, K., Hirashima, H., 2011. Study of a large-scale dry slab avalanche and the extent of damage to a cedar forest in the Makunosawa valley, Myoko, Japan. Ann. Glaciol. 52 (58), 119–128.

Teich, M., Bartelt, P., Grêt-Regamey, A., Bebi, P., 2012. Snow avalanches in forested terrain: influence of forest parameters, topography, and avalanche characteristics on runout distance. Arct. Antarct. Alp. Res. 44 (4), 509–519.

Teich, M., Fischer, J.-T., Feistl, T., Bebi, P., Christen, M., Grêt-Regamey, A., 2013a. Computational snow avalanche simulation in forested terrain. Natural Hazards and Earth System Science 14 (8), 2233–2248.

Teich, M., Techel, F., Caviezel, P., Bebi, P., 2013b. Forecasting forest avalanches: A review of winter 2011/12. In: Naaim-Bouvet, F., Durand, Y., Lambert, R. (Eds.), ISSW Proceedings, International Snow Science Workshop Grenoble – Chamonix Mont-Blanc - 2013, pp. 322–324.

Thiel, C., Schmullius, C., 2016. Comparison of UAV photograph-based and airborne lidar-based point clouds over forest from a forestry application perspective. Int. J. Remote Sens. 1366–5901.

Vacchiano, G., Maggioni, M., Perseghin, G., Motta, R., 2015. Effect of avalanche frequency on forest ecosystem services in spruce-fir mountain forest. Cold Reg. Sci. Technol. 115, 9–21.